Acknowledgment. We wish to thank the Science and Engineering Research Council for a studentship (to C.O.), Dr. N. El Murr (University of Dijon) for making the electrochemical measurements, and the National Science Foundation for financial support at Indiana University. We also thank Tim L. Davis, a participant in the 1981 IU High School Summer Science Institute, for the data on $ML_x(bpy)_y$ complexes.

Registry No. *cis*-$[Mo(bpy)_2(CO)_2]$, 29643-27-4; *cis*-$[Mo(CO)_2(phen)_2]$, 29643-29-6; *cis*-$[W(CO)_2(bpy)_2]$, 29643-28-5; $Mo(CO)_4(bpy)$, 15668-64-1; $Mo(CO)_4(phen)$, 15740-78-0; $W(CO)_4(bpy)$, 15668-66-3.

Supplementary Material Available: Listings of anisotropic thermal parameters and structure factor tables for the $Mo(bpy)_2(CO)_2$ molecule (17 pages). Ordering information is given on any current masthead page.

Contribution from the Department of Chemistry and Molecular Structure Center,
Indiana University, Bloomington, Indiana 47405

Reactions of Metal–Metal Multiple Bonds. 13.[1] Reactions of Diazoalkanes with Hexaalkoxides of Dimolybdenum and Ditungsten ($M{\equiv}M$). Preparation and Characterization of $Mo_2(O\text{-}i\text{-}Pr)_6(N_2CPh_2)_2(py)$, $W_2(O\text{-}t\text{-}Bu)_6(N_2C(p\text{-}tol)_2)_2$, and $Mo(O\text{-}t\text{-}Bu)_4(N_2CPh_2)$

MALCOLM H. CHISHOLM,* KIRSTEN FOLTING, JOHN C. HUFFMAN, and A. L. RATERMANN

Received August 18, 1983

Various aryl-substituted diazomethanes have been found to react with $M_2(OR)_6$ ($M{\equiv}M$) compounds in hydrocarbon solvents at room temperature. A variety of products are formed, depending on M (Mo or W) and the alkoxy ligand, but in no instance is there evidence of alkylidene formation. The dinuclear center serves as a source of electrons for the reduction of the diazoalkane to a 2– ligand, i.e. to a hydrazone-type NNCRR′ ligand. In the reaction between $Mo_2(O\text{-}t\text{-}Bu)_6$ and Ph_2CN_2 the $M{\equiv}M$ bond is cleaved, and the mononuclear compound $Mo(O\text{-}t\text{-}Bu)_4(NNCPh_2)$ has been isolated as a crystalline compound. The molecule has a trigonal-bipyramidal central MoO_4N moiety with short Mo–N (1.797 (3) Å) and long Mo–O (1.944 (3) Å) bonds in the axial positions. The equatorial Mo–O bond distances are 1.889 (3) Å (averaged). Related reactions involving $W_2(O\text{-}t\text{-}Bu)_6$ and Ar_2CN_2 yield $W_2(O\text{-}t\text{-}Bu)_6(\mu\text{-}NNCAr_2)_2$ compounds where Ar = Ph and *p*-tolyl (*p*-tol). The molecular structure of the *p*-tolyl derivative reveals a central $[O_3W\text{-}\mu\text{-}N]_2$ moiety based on the fusing of two trigonal-bipyramidal units sharing a common equatorial–axial edge formed by the agency of a pair of $NNCAr_2^{2-}$ ligands. The W–W and N–N distances are respectively 2.675 (1) and 1.410 (16) Å, indicative of single bonds. In the presence of donor ligands (pyridine or $HNMe_2$) the less sterically demanding isopropoxy and neopentoxy Mo_2 compounds form adducts of formula $Mo_2(OR)_6(N_2CAr_2)_2(L)$. The molecular structure of the compound $Mo_2(O\text{-}i\text{-}Pr)_6(NNCPh_2)_2(py)$ has three O-*i*-Pr ligands bridging a Mo–Mo single bond (2.662 (1) Å), with one terminal $NNCPh_2^{2-}$ ligand coordinated to each molybdenum atom. NMR and IR data are reported and the present results are compared and contrasted to related work involving mono- and dinuclear transition-metal complexes. Crystal data: for $Mo(O\text{-}t\text{-}Bu)_4(NNCPh_2)$, $a = 17.652$ (10) Å, $b = 12.366$ (6) Å, $c = 9.060$ (3) Å, $\alpha = 76.95$ (3)°, $\beta = 87.92$ (3)°, $\gamma = 124.92$ (2)°, $V = 1545$ (1) Å^3, $d_{calcd} = 1.252$ g cm^{-3}, and space group $P\bar{1}$; for $W_2(O\text{-}t\text{-}Bu)_6(NNC(p\text{-}tol)_2)_2$(hexane), $a = 23.672$ (5) Å, $b = 12.214$ (2) Å, $c = 21.221$ (6) Å, $\beta = 97.24$ (1)°, $V = 6086$ (1) Å^3, $d_{calcd} = 1.459$ g cm^{-3}, and space group $C2/c$; for $Mo_2(O\text{-}i\text{-}Pr)_6(NNCPh_2)_2(py)$, $a = 12.512$ (8) Å, $b = 14.795$ (9) Å, $c = 14.099$ (8) Å, $\beta = 109.51$ (2)°, $V = 2460$ (1) Å^3, $d_{calcd} = 1.369$ g cm^{-3}, and space group $P2_1$.

Introduction

Various transition metals are known to catalytically decompose diazomethane to polymethylene or ethylene.[2] Silver oxide, copper powder, and copper salts are also used in the catalytic formation of carbenes from diazoalkanes in organic syntheses. Diazoalkane metal complexes have been synthesized by reactions involving coordinated dinitrogen ligands with *gem*-dihalides,[3] acids,[4] and ketones[5] and by ligand displacement or substitution reactions involving the direct interaction between a diazoalkane and an unsaturated metal center.[6] Examples of the latter are reactions involving dinuclear compounds such as $Cp_2Mo_2(CO)_4$, which contains a $Mo{\equiv}Mo$ bond and yields various adducts depending upon the diazoalkane.[7] Diazoalkane complexes are often the precursors to metal alkylidene complexes by the thermally or photochemically induced elimination of dinitrogen. As part of a continuing study of the chemistry of $(RO)_3M{\equiv}M(OR)_3$ compounds, where M = Mo and W,[8] we describe here our studies of their reactions with aryl-substituted diazomethanes. A preliminary report of a part of this study has appeared.[9]

Results and Discussions

Syntheses. The isolated new diazoalkane compounds have been obtained from the reactions shown in eq 1–3.

---

(1) Part 12: Chisholm, M. H.; Huffman, J. C.; Ratermann, A. L.; Smith, C. *Inorg. Chem.* **1984**, *23*, 1596.

(2) Kirmse, W. "Carbene Chemistry"; Academic Press: New York, 1964.

(3) Ben-Shoshan, R.; Chatt, J.; Hussain, W.; Leigh, G. J. *J. Organomet. Chem.* **1976**, *112*, C9.

(4) Bevan, P. C.; Chatt, J.; Hidai, M.; Leigh, G. J. *J. Organomet. Chem.* **1978**, *160*, 165.

(5) Hidai, M.; Mizobe, Y.; Vehida, Y. *J. Am. Chem. Soc.* **1976**, *98*, 7824.

(6) For a recent review of transition-metal diazoalkane complexes, see: Hermann, W. A. *Angew. Chem., Int. Ed. Engl.* **1978**, *17*, 800.

(7) (a) Messerle, L.; Curtis, M. D. *J. Am. Chem. Soc.* **1980**, *102*, 7789. (b) *Ibid.* **1982**, *104*, 889. (c) D'Errico, J. J.; Messerle, L.; Curtis, M. D. *Inorg. Chem.* **1983**, *22*, 849.

(8) Chisholm, M. H. *Polyhedron* **1983**, *2*, 681.

(9) Chisholm, M. H.; Folting, K.; Huffman, J. C.; Ratermann, A. L. *J. Chem. Soc., Chem. Commun.* **1981**, 1229.

0020-1669/84/1323-2303$01.50/0

$$\mathrm{Mo_2(OR)_6} + 2\mathrm{R'R''CN_2} \xrightarrow[\text{hexane}]{\text{excess L}} \mathrm{Mo_2(OR)_6(NNCR'R'')_2L} \quad (1)$$

R	R′	R″	L
i-Pr	Ph	Ph	py
CH_2-*t*-Bu	Ph	Ph	py
CH_2-*t*-Bu	Ph	H	py
CH_2-*t*-Bu	Ph	Ph	$HNMe_2$

$$\mathrm{W_2(O\text{-}\mathit{t}\text{-}Bu)_6} + 2\mathrm{R_2CN_2} \xrightarrow[\text{hexane}]{} \mathrm{W_2(O\text{-}\mathit{t}\text{-}Bu)_6(NNCR_2)_2} \quad (2)$$

R = Ph and *p*-tolyl

$$\mathrm{Mo_2(O\text{-}\mathit{t}\text{-}Bu)_6} + 2\mathrm{Ph_2CN_2} \xrightarrow[\text{hexane}]{} \mathrm{Mo(O\text{-}\mathit{t}\text{-}Bu)_4(NNCPh_2)} \quad (3)$$

The diazoalkanes react rapidly with hydrocarbon solutions of $M_2(OR)_6$ compounds even at low temperatures (−78 °C). From the isolated compounds and from NMR studies of ^{13}C-labeled $Ar_2{}^*CN_2$ compounds, we have found no evidence of alkylidene formation or products that could be inferred as being derived from the formation of a reactive carbene intermediate. The basic course of the reaction appears to be one in which the six electrons of the M≡M bond are used to reduce the diazoalkane to a 2− ligand. The initial reaction is very fast, producing $M_2(OR)_6(NNCAr_2)_2$ compounds, which in the case of M = W and R = *t*-Bu are isolable. For molybdenum, isolable adducts of this type are obtained when the alkoxy group is less bulky provided an additional donor ligand, py or $HNMe_2$, is present. Addition of only 1 equiv of diazoalkane yields a 1:1 mixture of $Mo_2(OR)_6$ and $Mo_2(OR)_6(NNCAr_2)_2(L)$. In the case of L = $HNMe_2$, which is labile, further reaction with diazoalkane occurs and we believe the remaining two electrons of the M–M bond are used to yield $Mo(OR)_4(NNCAr_2)$ and $Mo(OR)_2(NNCAr_2)_2$ compounds. This would parallel reactions involving $Mo_2(OR)_6$ compounds and molecular oxygen, which yield $MoO_2(OR)_2$ and $MoO(OR)_4$ compounds.[10] However, we have not been able to isolate any compound of formula $Mo(OR)_2(NNCAr_2)_2$, and only the compound Mo(O-*t*-Bu)$_4$(NNCAr$_2$) testifies to the total destruction of the M–M bond. One of the synthetic problems in this work has been the difficulty in obtaining crystalline materials that are readily characterized. The compounds tend to be extremely soluble in hydrocarbon solvents. However, the general pattern of reactivity can reasonably be inferred from the characterized products of reactions 1–3. In all instances the dinuclear center provides a reservoir of electrons for reduction of the diazoalkane to a 2–ligand, a hydrazone-type ligand. It may be noted that bis(imido) compounds Mo(O-*t*-Bu)$_2$(NAr)$_2$, which are isoelectronic with the proposed $Mo(OR)_2(NNCAr_2)_2$ compounds, have been isolated from reactions involving Mo$_2$(O-*t*-Bu)$_6$ and ArN_3 (Ar = Ph, *p*-tol).[11]

Molecular Structures and Bonding Considerations. Mo(O-*t*-Bu)$_4$(NNCPh$_2$). Fractional coordinates are given in Table I, and selected bond distances and bond angles are given in Tables II and III, respectively. An ORTEP view of the molecule giving the atom-number scheme used in the tables is shown in Figure 1.

The coordination geometry about molybdenum is close to that of an idealized trigonal bipyramid. The trans N–Mo–O angle is 177.1 (1)° and the sum of the three equatorial O–Mo–O angles (115.2 (1), 126.1 (1), and 117.2 (1)°) is 358.5°.

Table I. Fractional Coordinates and Isotropic Thermal Parameters for the Mo(O-*t*-Bu)$_4$(NNCPh$_2$) Molecule

atom	10^4x	10^4y	10^4z	$10B_{iso}$, Å^2
Mo(1)	7056.2 (2)	4358.3 (4)	5403.4 (4)	12
N(2)	7515 (2)	6113 (3)	4405 (4)	14
N(3)	7909 (2)	7349 (3)	3433 (4)	15
C(4)	7978 (3)	8345 (4)	3854 (5)	16
C(5)	8430 (3)	9670 (4)	2608 (5)	14
C(6)	9095 (3)	10044 (4)	1345 (5)	21
C(7)	9491 (3)	11263 (5)	158 (5)	23
C(8)	9222 (3)	12097 (4)	203 (5)	22
C(9)	8557 (3)	11735 (4)	1439 (5)	20
C(10)	8177 (3)	10541 (4)	2625 (5)	18
C(11)	7662 (3)	8236 (4)	5454 (5)	16
C(12)	6807 (3)	7076 (4)	6404 (5)	18
C(13)	6543 (3)	7001 (5)	7892 (5)	24
C(14)	7148 (4)	8068 (5)	8485 (5)	30
C(15)	7990 (4)	9221 (5)	7572 (5)	29
C(16)	8247 (3)	9308 (4)	6078 (5)	21
O(17)	5936 (2)	4023 (3)	6359 (3)	17
C(18)	4987 (3)	2802 (4)	7154 (5)	18
C(19)	4414 (3)	3360 (5)	7241 (5)	23
C(20)	4610 (3)	1819 (5)	6198 (6)	28
C(21)	5009 (3)	2157 (5)	8767 (5)	26
O(22)	6967 (2)	3760 (3)	3647 (3)	15
C(23)	7104 (3)	4312 (4)	1991 (5)	20
C(24)	6845 (3)	3135 (5)	1344 (5)	25
C(25)	6452 (4)	4716 (6)	1673 (6)	35
C(26)	8125 (4)	5508 (5)	1345 (6)	35
O(27)	8125 (2)	4847 (3)	6281 (3)	17
C(28)	9088 (3)	6053 (4)	6108 (5)	18
C(29)	9515 (3)	5507 (5)	7166 (6)	29
C(30)	9095 (3)	7151 (5)	6602 (5)	22
C(31)	9594 (3)	6593 (5)	4435 (6)	26
O(32)	6573 (2)	2486 (3)	6578 (3)	16
C(33)	6821 (3)	1552 (4)	6833 (5)	20
C(34)	7599 (3)	2012 (5)	5514 (6)	28
C(35)	5942 (4)	135 (5)	6938 (6)	29
C(36)	7157 (3)	1552 (5)	8348 (6)	25

Table II. Bond Distances (Å) for the Mo(O-*t*-Bu)$_4$(NNCPh$_2$) Molecule

A	B	dist	A	B	dist
Mo(1)	O(17)	1.899 (3)	C(11)	C(12)	1.395 (6)
Mo(1)	O(22)	1.876 (3)	C(11)	C(16)	1.398 (6)
Mo(1)	O(27)	1.892 (3)	C(12)	C(13)	1.375 (6)
Mo(1)	O(32)	1.944 (3)	C(13)	C(14)	1.385 (7)
Mo(1)	N(2)	1.797 (3)	C(14)	C(15)	1.370 (7)
O(17)	C(18)	1.460 (5)	C(15)	C(16)	1.373 (6)
O(22)	C(23)	1.448 (5)	C(18)	C(19)	1.524 (6)
O(27)	C(28)	1.453 (5)	C(18)	C(20)	1.504 (7)
O(32)	C(33)	1.431 (5)	C(18)	C(21)	1.512 (6)
N(2)	N(3)	1.314 (4)	C(23)	C(24)	1.521 (6)
N(3)	C(4)	1.312 (5)	C(23)	C(25)	1.508 (7)
C(4)	C(5)	1.482 (6)	C(23)	C(26)	1.503 (7)
C(4)	C(11)	1.483 (6)	C(28)	C(29)	1.512 (7)
C(5)	C(6)	1.393 (6)	C(28)	C(30)	1.517 (6)
C(5)	C(10)	1.386 (6)	C(28)	C(31)	1.518 (7)
C(6)	C(7)	1.387 (6)	C(33)	C(34)	1.522 (7)
C(7)	C(8)	1.367 (6)	C(33)	C(35)	1.512 (7)
C(8)	C(9)	1.381 (6)	C(33)	C(36)	1.515 (7)
C(9)	C(10)	1.372 (6)			

The distortions from an idealized C_{3v} structure for the central MoO_4N moiety can readily be understood in terms of the fact that the positioning of the CPh_2 group distroys the possibility of C_3 symmetry. Also the N–Mo–O angles are slightly greater than 90° (90.6 (1), 97.2 (1), and 94.7 (1)°), probably as a result of a higher degree of multiple-bond order in the Mo–N bond relative to the trans Mo–OR bond. This is also born out by the fact that the Mo–O equatorial bond distances, 1.89 Å (averaged), are significantly shorter than the axial Mo–O bond distance, 1.944 (3) Å. The Mo–N distance of 1.797 (3) Å is clearly indicative of N–Mo multiple-bond order. It is,

---

(10) Chisholm, M. H.; Folting, K.; Huffman, J. C.; Kirkpatrick, C. C. *Inorg. Chem.* **1984**, *23*, 1021.

(11) Chisholm, M. H.; Folting, K.; Huffman, J. C.; Ratermann, A. L. *Inorg. Chem.* **1982**, *21*, 978.

Table III. Selected Bond Angles (deg) for the $Mo(O\text{-}t\text{-}Bu)_4(NNCPh_2)$ Molecule

A	B	C	angle
O(17)	Mo(1)	O(22)	115.2 (1)
O(17)	Mo(1)	O(27)	126.1 (1)
O(17)	Mo(1)	O(32)	88.6 (1)
O(17)	Mo(1)	N(2)	90.6 (1)
O(22)	Mo(1)	O(27)	117.2 (1)
O(22)	Mo(1)	O(32)	85.6 (1)
O(22)	Mo(1)	N(2)	97.2 (1)
O(27)	Mo(1)	O(32)	83.6 (1)
O(27)	Mo(1)	N(2)	94.7 (1)
O(32)	Mo(1)	N(2)	177.1 (1)
Mo(1)	O(17)	C(18)	135.9 (2)
Mo(1)	O(22)	C(23)	137.7 (2)
Mo(1)	O(27)	C(28)	138.8 (2)
Mo(1)	O(32)	C(33)	141.4 (2)
Mo(1)	N(2)	N(3)	168.2 (3)
N(2)	N(3)	C(4)	122.5 (3)
N(3)	C(4)	C(5)	115.6 (3)
N(3)	C(4)	C(11)	124.9 (4)

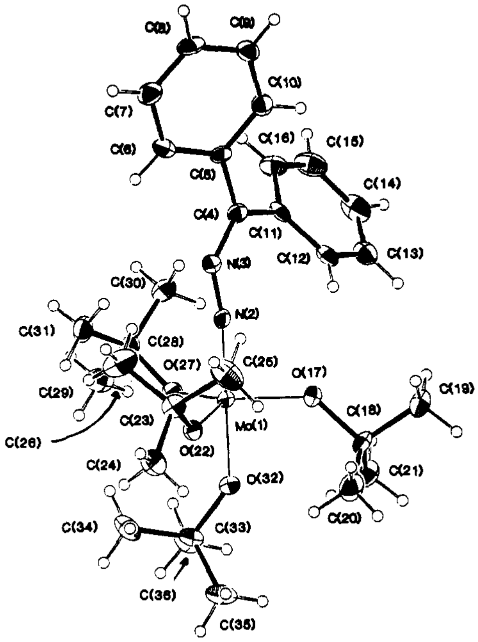

Figure 1. ORTEP view of the $Mo(O\text{-}t\text{-}Bu)_4(NNCPh_2)$ molecule giving the atom-number scheme used in the tables.

however, longer than might be expected[12] for a Mo–N triple bond, 1.71 Å.

An interesting comparison of M–O and M–N distances can be made with the trigonal-bipyramidal molecules $W(O\text{-}t\text{-}Bu)_3(NO)(py)$[13] and $[(t\text{-}BuO)_3W{\equiv}N]_x$,[14] bearing in mind Mo–L and W–L bond distances in related compounds differ by less than 0.01 or 0.02 Å. In $W(O\text{-}t\text{-}Bu)_3(NO)(py)$ the nitrosyl and pyridine ligands occupy axial positions with W–N distances of 1.732 (7) and 2.323 (7) Å, respectively. The W–O equatorial bond distances average 1.89 Å and are bent away from the axial nitrosyl ligand, ON–W–O = 112 (1)° (averaged). The structure of the nitride is an interesting linear polymer based on alternating short, 1.740 (15) Å, and long, 2.66 (1) Å, W–N distances corresponding to W–N triple and weak dative bonds, respectively. There is a crystallographically imposed C_3 axis of symmetry coincident with the $N{-}{-}{-}W{\equiv}N$ axis, and the W–O bonds, 1.872 (7) Å, are again bent back from the W–N multiple bond, N–W–O = 101.6 (1)°. Thus the only significant differences in the present molecule can be understood in terms of π-bonding competition between the axial $NNCAr_2$ and OR ligands.

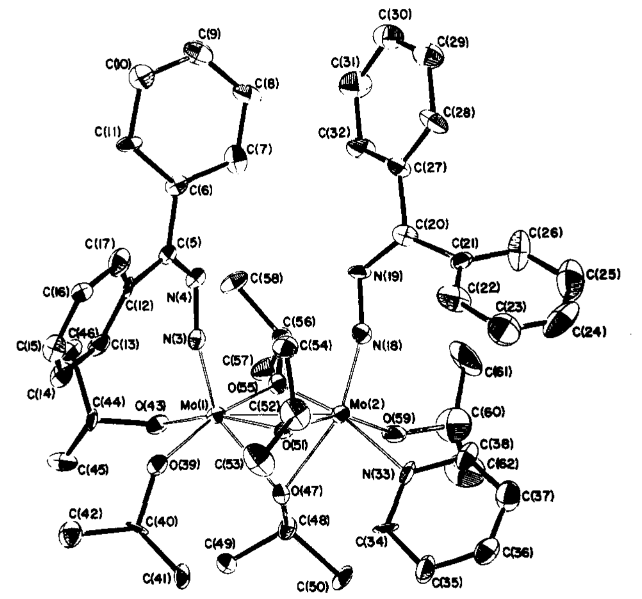

Figure 2. ORTEP view of the $Mo_2(O\text{-}i\text{-}Pr)_6(NNCPh_2)_2(py)$ molecule giving the atom-number scheme used in the tables.

In a trigonal-bipyramidal geometry, molybdenum may use s, p_x, p_y, p_z, and d_{z^2} orbitals to form five σ bonds. If the $NNCAr_2$ ligand is counted as a 2– ligand, then vacant Mo d_{xz} and d_{yz} atomic orbitals are available to receive π electrons from both the imido and alkoxy axial ligands. In the xy plane, molybdenum atomic orbitals, $d_{x^2-y^2}$ and d_{xy}, may be involved in π-bonding with the equatorial OR ligands. Thus, as a result of forming M–L σ and π bonds, molybdenum can attain an 18-electron configuration. In terms of resonance structures the axial ligands have a contribution from both I and II.

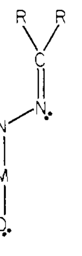

I

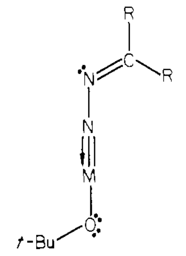

II

Consequently, the Mo–N and Mo–O (axial) bonds are somewhat longer than they would be if they were triple and double bonds, respectively.

$Mo_2(O\text{-}i\text{-}Pr)_6(NNCPh_2)_2(py)$. Fractional coordinates are given in Table IV. Selected bond distances and bond angles are given in Tables V and VI, respectively. An ORTEP view of the molecule giving the atom-number scheme is shown in Figure 2.

Each molybdenum is in a distorted octahedral environment, and the halves of the molecule share a face formed by three bridging O-*i*-Pr ligands. The molecule has no symmetry, and the distortions from an idealized confacial bioctahedral geometry for the $Mo_2O_6N_3$ moiety may be understood in terms of electronic and steric factors.

The Mo–Mo distance of 2.661 (2) Å is consistent with a single bond; cf.[15] Mo–Mo = 2.73 Å in edge-shared biocta-

---

(12) Nugent, W. A.; Haymore, B. L. *Coord. Chem. Rev.* **1980**, *31*, 123.

(13) Chisholm, M. H.; Cotton, F. A.; Extine, M. W.; Kelly, R. L. *Inorg. Chem.* **1979**, *18*, 116.

(14) Chisholm, M. H.; Hoffman, D. M.; Huffman, J. C. *Inorg. Chem.* **1983**, *22*, 2903.

(15) Chisholm, M. H.; Huffman, J. C.; Kirkpatrick, C. C. *Inorg. Chem.* **1981**, *20*, 871.

Table IV. Fractional Coordinates and Isotropic Thermal Parameters for the $Mo_2(O\text{-}i\text{-}Pr)_6(NNCPh_2)_2(py)$ Molecule

atom	10^4x	10^4y	10^4z	$10B_{iso}$, Å^2
Mo(1)	1109 (1)	2642[a]	7163 (1)	12
Mo(2)	3305 (1)	2917 (1)	7487 (1)	12
N(3)	1065 (7)	2299 (6)	8344 (7)	13
N(4)	1276 (7)	2186 (6)	9317 (7)	14
C(5)	951 (9)	1492 (8)	9700 (8)	16
C(6)	1339 (9)	1540 (7)	10815 (8)	13
C(7)	2425 (10)	1931 (8)	11326 (9)	21
C(8)	2829 (10)	1980 (9)	12377 (8)	23
C(9)	2142 (11)	1683 (8)	12921 (9)	24
C(10)	1102 (10)	1318 (8)	12447 (9)	22
C(11)	672 (10)	1234 (8)	11382 (8)	17
C(12)	247 (8)	720 (7)	9161 (8)	13
C(13)	−498 (10)	822 (8)	8164 (9)	18
C(14)	−1168 (10)	109 (8)	7670 (9)	20
C(15)	−1079 (10)	−733 (9)	8168 (9)	24
C(16)	9628 (10)	9169 (9)	9140 (9)	19
C(17)	288 (10)	−111 (9)	9628 (9)	23
N(18)	3970 (7)	2808 (6)	8813 (6)	15
N(19)	4110 (7)	2973 (7)	9751 (6)	18
C(20)	5068 (9)	2795 (8)	10466 (7)	18
C(21)	6058 (10)	2404 (8)	10266 (8)	18
C(22)	5922 (12)	1571 (10)	9749 (10)	33
C(23)	6776 (13)	1193 (12)	9428 (11)	43
C(24)	7752 (14)	1675 (12)	9688 (12)	48
C(25)	7937 (12)	2484 (12)	10234 (12)	47
C(26)	7067 (10)	2827 (10)	10526 (11)	36
C(27)	5140 (9)	3120 (8)	11490 (8)	21
C(28)	5962 (10)	2730 (9)	12346 (8)	26
C(29)	6028 (10)	3040 (9)	13310 (9)	27
C(30)	5298 (11)	3709 (9)	13421 (9)	28
C(31)	4488 (12)	4089 (10)	12561 (10)	31
C(32)	4422 (10)	3786 (9)	11622 (9)	23
N(33)	4413 (7)	2150 (7)	6819 (7)	18
C(34)	3906 (10)	1705 (8)	5950 (8)	19
C(35)	4545 (10)	1218 (10)	5472 (10)	27
C(36)	5725 (10)	1214 (9)	5913 (9)	24
C(37)	6223 (11)	1685 (10)	6779 (10)	30
C(38)	5554 (10)	2145 (8)	7243 (9)	21
O(39)	20 (6)	1770 (5)	6321 (6)	16
C(40)	−571 (10)	1866 (8)	5263 (8)	18
C(41)	136 (9)	1461 (9)	4676 (9)	20
C(42)	−1712 (10)	1385 (9)	5043 (9)	23
O(43)	−100 (6)	3556 (5)	6766 (5)	16
C(44)	−1240 (9)	3406 (8)	6682 (8)	15
C(45)	−1990 (11)	4001 (10)	5874 (9)	30
C(46)	−1412 (10)	3636 (10)	7700 (9)	25
O(47)	1966 (5)	3015 (5)	6055 (5)	14
C(48)	1846 (10)	3802 (8)	5441 (8)	18
C(49)	627 (10)	3877 (9)	4716 (8)	19
C(50)	2674 (10)	3743 (9)	4833 (9)	23
O(51)	2426 (6)	1725 (5)	7223 (5)	14
C(52)	2793 (11)	835 (8)	7592 (10)	27
C(53)	2092 (12)	157 (9)	6847 (11)	34
C(54)	2867 (11)	657 (9)	8640 (9)	24
O(55)	2148 (6)	3797 (5)	7693 (5)	14
C(56)	2284 (9)	4545 (7)	8356 (8)	15
C(57)	1842 (13)	5377 (10)	7738 (10)	34
C(58)	1640 (11)	4347 (9)	9113 (9)	22
O(59)	4035 (7)	4027 (6)	7193 (6)	27
C(60)	5096 (15)	4355 (12)	7455 (12)	50
C(61)	5472 (14)	4778 (14)	8481 (12)	60
C(62)	5044 (16)	5140 (12)	6681 (12)	58

[a] Parameter not varied.

Table V. Selected Bond Distances (Å) for the $Mo_2(O\text{-}i\text{-}Pr)_6(NNCPh_2)_2(py)$ Molecule

A	B	dist	A	B	dist
Mo(1)	Mo(2)	2.662 (2)	O(39)	C(40)	1.433 (13)
Mo(1)	O(39)	1.962 (7)	O(43)	C(44)	1.409 (13)
Mo(1)	O(43)	1.966 (7)	O(47)	C(48)	1.429 (14)
Mo(1)	O(47)	2.239 (7)	O(51)	C(52)	1.433 (15)
Mo(1)	O(51)	2.114 (7)	O(55)	C(56)	1.421 (13)
Mo(1)	O(55)	2.127 (7)	O(59)	C(60)	1.344 (17)
Mo(1)	N(3)	1.758 (9)	N(3)	N(4)	1.319 (12)
Mo(2)	O(47)	2.155 (7)	N(4)	C(5)	1.287 (14)
Mo(2)	O(51)	2.046 (8)	N(18)	N(19)	1.297 (11)
Mo(2)	O(55)	2.040 (7)	N(19)	C(20)	1.310 (13)
Mo(2)	O(59)	1.989 (8)	N(33)	C(34)	1.349 (14)
Mo(2)	N(18)	1.781 (8)	N(33)	C(38)	1.351 (15)
Mo(2)	N(33)	2.229 (9)			

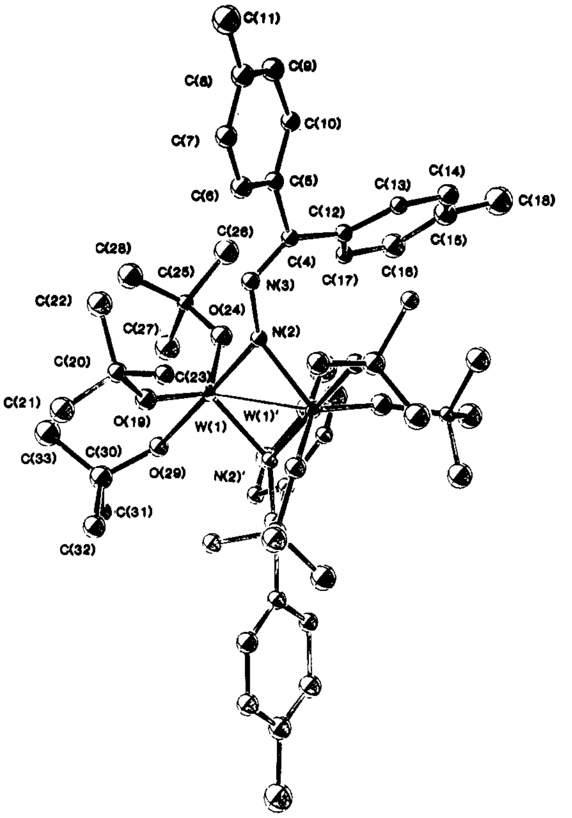

Figure 3. ORTEP view of the $W_2(O\text{-}t\text{-}Bu)_6(NNC(p\text{-}tolyl)_2)_2$ molecule giving the atom-number scheme used in the tables. Atoms related by the C_2 axis of symmetry are denoted by a prime.

hedral complexes $Mo_2(O\text{-}i\text{-}Pr)_6X_4$, where X = Cl and Br. This is consistent with the presence of a central Mo_2^{10+} unit with terminal $NNCAr_2^{2-}$ ligands. In a formal sense this compound contains metal atoms in differing oxidation states: $+5^1/_2$ for Mo(1) and $+4^1/_2$ for Mo(2). This charge imbalance is offset by the formation of asymmetric alkoxide bridges that have shorter Mo–O distances to Mo(2) than to Mo(1) and by subtle differences in the bonding of the $NNCPh_2$ ligands as indicated by Mo–N distances and Mo–N–N angles. The ligands that are cis to the $NNCPh_2$ group are bent away very slightly (1–15°), presumably as a result of combined steric factors and the M–N multiple bond. After forming a M–M σ bond, each molybdenum has two t_{2g} type atomic orbitals available (empty) for π-bonding with the $NNCPh_2$ and OR ligands. Again the Mo–N distances, 1.76 and 1.78 Å, and the bent Mo–N–N moiety imply an intermediate mode of bonding, somewhere between I and II, for the Mo–$NNCPh_2$ group.

$W_2(O\text{-}t\text{-}Bu)_6(NNC(C_6H_4Me)_2)_2$. Fractional coordinates are given in Table VII. Selected bond distances and bond angles are given in Tables VIII and IX, respectively. An ORTEP view of the $W_2(O\text{-}t\text{-}Bu)_6(NNC(C_6H_4Me)_2)_2$ molecule giving the atom-number scheme used in the tables is given in Figure 3.

Each tungsten atom is in a distorted trigonal-bipyramidal environment, and the halves of the molecule are joined along a common axial–equatorial edge by a pair of μ-NNC(tol)$_2$ ligands. This compound is a member of a now fairly extensive class of compounds based on fused trigonal bipyramids sharing axial–equatorial edges, which includes $Mo_2(O\text{-}i\text{-}Pr)_8$ (M=

Table VI. Selected Bond Angles (deg) for the $Mo_2(O\text{-}i\text{-}Pr)_6(NNCPh_2)_2(py)$ Molecule

A	B	C	angle
Mo(2)	Mo(1)	O(39)	132.2 (2)
Mo(2)	Mo(1)	O(43)	126.5 (2)
Mo(2)	Mo(1)	O(47)	51.3 (2)
Mo(2)	Mo(1)	O(51)	49.1 (2)
Mo(2)	Mo(1)	O(55)	48.9 (2)
Mo(2)	Mo(1)	N(3)	103.8 (3)
O(39)	Mo(1)	O(43)	88.1 (3)
O(39)	Mo(1)	O(47)	97.9 (3)
O(39)	Mo(1)	O(51)	88.7 (3)
O(39)	Mo(1)	O(55)	163.9 (3)
O(39)	Mo(1)	N(3)	98.6 (4)
O(43)	Mo(1)	O(47)	97.7 (3)
O(43)	Mo(1)	O(51)	165.5 (3)
O(43)	Mo(1)	O(55)	82.4 (3)
O(43)	Mo(1)	N(3)	101.7 (3)
O(47)	Mo(1)	O(51)	68.8 (3)
O(47)	Mo(1)	O(55)	70.6 (3)
O(47)	Mo(1)	N(3)	154.8 (3)
O(51)	Mo(1)	O(55)	97.2 (3)
O(51)	Mo(1)	N(3)	92.7 (3)
O(55)	Mo(1)	N(3)	96.1 (3)
Mo(1)	Mo(2)	O(47)	54.2 (2)
Mo(1)	Mo(2)	O(51)	51.4 (2)
Mo(1)	Mo(2)	O(55)	51.8 (2)
Mo(1)	Mo(2)	O(59)	127.6 (3)
Mo(1)	Mo(2)	N(18)	105.1 (3)
Mo(1)	Mo(2)	N(33)	127.0 (3)
O(47)	Mo(2)	O(51)	71.6 (3)
O(47)	Mo(2)	O(55)	74.0 (3)
O(47)	Mo(2)	O(59)	90.9 (3)
O(47)	Mo(2)	N(18)	159.0 (3)
O(47)	Mo(2)	N(33)	92.1 (3)
O(51)	Mo(2)	O(55)	102.3 (3)
O(51)	Mo(2)	O(59)	158.5 (3)
O(51)	Mo(2)	N(18)	98.5 (4)
O(51)	Mo(2)	N(33)	81.8 (3)
O(55)	Mo(2)	O(59)	84.2 (3)
O(55)	Mo(2)	N(18)	90.8 (3)
O(55)	Mo(2)	N(33)	163.1 (3)
O(59)	Mo(2)	N(18)	102.0 (4)
O(59)	Mo(2)	N(33)	86.5 (4)
N(18)	Mo(2)	N(33)	105.0 (4)
Mo(1)	O(39)	C(40)	125.2 (7)
Mo(1)	O(43)	C(44)	125.2 (7)
Mo(1)	O(47)	Mo(2)	74.6 (2)
Mo(1)	O(47)	C(48)	130.3 (6)
Mo(2)	O(47)	C(48)	120.9 (6)
Mo(1)	O(51)	Mo(2)	79.6 (3)
Mo(1)	O(51)	C(52)	139.0 (7)
Mo(2)	O(51)	C(52)	129.7 (7)
Mo(1)	O(55)	Mo(2)	79.4 (3)
Mo(1)	O(55)	C(56)	141.4 (6)
Mo(2)	O(55)	C(56)	131.0 (6)
Mo(2)	O(59)	C(60)	136.1 (10)
Mo(1)	N(3)	N(4)	164.4 (8)
N(3)	N(4)	C(5)	123.8 (9)
Mo(2)	N(18)	N(19)	155.3 (7)
N(18)	N(19)	C(20)	121.6 (9)
Mo(2)	N(33)	C(34)	117.5 (7)
Mo(2)	N(33)	C(38)	122.0 (8)

Table VII. Fractional Coordinates and Isotropic Thermal Parameters for the $W_2(O\text{-}t\text{-}Bu)_6(NNC(p\text{-tol})_2)_2$ Molecule

atom	10^4x	10^4y	10^4z	$10B_{iso}$, Å^2
W(1)	−270.2 (3)	1775 (1)	3016.9 (3)	11
N(2)	546 (5)	1872 (10)	2883 (5)	11 (2)
N(3)	1077 (5)	1793 (11)	3263 (5)	13 (2)
C(4)	1455 (6)	2520 (12)	3245 (7)	12 (3)
C(5)	2005 (6)	2257 (13)	3661 (7)	14 (3)
C(6)	2172 (7)	1185 (13)	3777 (7)	19 (3)
C(7)	2661 (7)	938 (13)	4157 (7)	19 (3)
C(8)	3012 (6)	1764 (15)	4458 (7)	20 (3)
C(9)	2842 (7)	2802 (13)	4359 (8)	20 (3)
C(10)	2347 (6)	3073 (13)	3955 (7)	14 (3)
C(11)	3558 (8)	1461 (15)	4861 (9)	31 (4)
C(12)	1411 (6)	3602 (12)	2935 (7)	12 (3)
C(13)	1872 (6)	4023 (12)	2647 (7)	12 (3)
C(14)	1872 (7)	5057 (13)	2398 (7)	18 (3)
C(15)	1400 (7)	5733 (14)	2415 (8)	22 (3)
C(16)	921 (7)	5301 (14)	2652 (8)	22 (3)
C(17)	932 (6)	4268 (12)	2905 (7)	11 (3)
C(18)	1392 (7)	6889 (16)	2161 (8)	31 (4)
O(19)	−176 (4)	368 (9)	3366 (5)	18 (2)
C(20)	231 (6)	−448 (13)	3660 (7)	15 (3)
C(21)	−91 (7)	−1433 (14)	3819 (18)	25 (4)
C(22)	567 (7)	53 (14)	4264 (8)	25 (4)
C(23)	650 (6)	−748 (13)	3181 (7)	15 (3)
O(24)	−209 (4)	3136 (9)	3410 (5)	18 (2)
C(25)	−342 (6)	3649 (12)	3993 (7)	10 (3)
C(26)	−28 (7)	4745 (15)	4052 (8)	24 (4)
C(27)	−986 (7)	3870 (14)	3942 (8)	24 (4)
C(28)	−145 (7)	2919 (14)	4540 (8)	24 (4)
O(29)	−1060 (4)	1613 (8)	3162 (4)	15 (2)
C(30)	−1464 (7)	945 (14)	3423 (8)	21 (3)
C(31)	−2049 (6)	1575 (12)	3313 (7)	14 (3)
C(32)	−1539 (7)	−132 (13)	3064 (8)	20 (3)
C(33)	−1321 (7)	762 (14)	4128 (8)	26 (4)
C(34)	3518 (14)	1654 (29)	801 (16)	94 (9)
C(35)	3151 (11)	2473 (21)	606 (12)	57 (6)
C(36)	2721 (10)	2076 (19)	101 (11)	53 (5)

Table VIII. Selected Bond Distances (Å) for the $W_2(O\text{-}t\text{-}Bu)_6(NNC(p\text{-tol})_2)_2$ Molecule

A	B	dist	A	B	dist
W(1)	W(1)′	2.675 (1)	O(19)	C(20)	1.468 (18)
W(1)	O(19)	1.874 (11)	O(24)	C(25)	1.455 (18)
W(1)	O(24)	1.858 (11)	O(29)	C(30)	1.420 (19)
W(1)	O(29)	1.944 (9)	N(2)	N(3)	1.410 (16)
W(1)	N(2)	1.942 (11)	N(3)	C(4)	1.264 (18)
W(1)	N(2)′	1.991 (11)			

Table IX. Selected Bond Angles (deg) for the $W_2(O\text{-}t\text{-}Bu)_6(NNC(p\text{-tol})_2)_2$ Molecule

A	B	C	angle
W(1)′	W(1)	O(19)	106.2 (3)
W(1)′	W(1)	O(24)	110.5 (3)
W(1)′	W(1)	O(29)	134.4 (3)
W(1)′	W(1)	N(2)	47.9 (3)
O(19)	W(1)	O(24)	130.1 (4)
O(19)	W(1)	O(29)	85.0 (4)
O(19)	W(1)	N(2)	117.0 (5)
O(24)	W(1)	O(29)	92.4 (4)
O(24)	W(1)	N(2)	89.3 (5)
O(29)	W(1)	N(2)	177.4 (4)
N(2)	W(1)	N(2)′	93.9 (4)
W(1)	O(19)	C(20)	146.0 (9)
W(1)	O(24)	C(25)	138.9 (9)
W(1)	O(29)	C(30)	145.9 (9)
W(1)	N(2)	W(1)′	85.7 (4)
W(1)	N(2)	N(3)	136.6 (9)
N(2)	N(3)	C(4)	121.2 (13)

M),[16] $[(i\text{-PrO})_2(NO)Mo(\mu\text{-}O\text{-}i\text{-}Pr)]_2$,[17] $[(t\text{-BuO})_2(ArN)Mo(\mu\text{-}NAr)]_2$.[11,18] In $Mo_2(O\text{-}i\text{-}Pr)_8$ there is a Mo–Mo double bond of distance 2.525 (1) Å, while in the last two compounds there are nonbonding M–M distances >3.2 Å. In the present molecule the W–W distance is 2.675 (1) Å, which may be taken as a single-bond distance consistent with the formulation of the bridging diazoalkanes as 2− ligands. As with the fused trigonal-bipyramidal molecules, the metal–axial bond distances are longer than the metal–equatorial distances. This, taken with the N–N distance, 1.410 (16) Å, and the N–N–C angle

---

(16) Chisholm, M. H.; Cotton, F. A.; extine, M. W.; Reichert, W. W. *Inorg. Chem.* **1978**, *17*, 2944.

(17) Chisholm, M. H.; Cotton, F. A.; Extine, M. W.; Kelly, R. L. *J. Am. Chem. Soc.* **1978**, *100*, 3354.

(18) Chisholm, M. H.; Folting, K.; Huffman, J. C.; Kirkpatrick, C. C.; Ratermann, A. L. *J. Am. Chem. Soc.* **1981**, *103*, 1305.

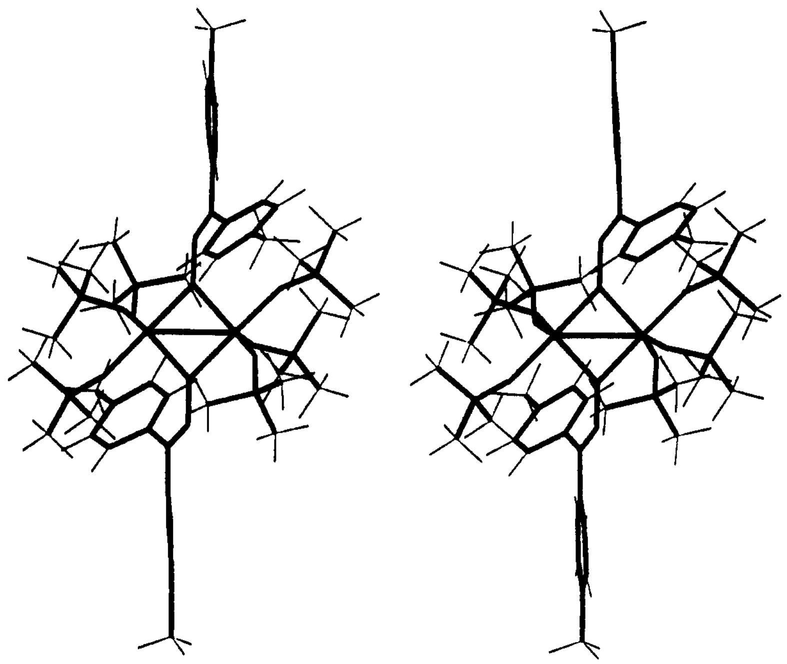

Figure 4. Stick stereoview of the $W_2(O\text{-}t\text{-}Bu)_6(NNC)p\text{-}tol)_2)_2$ molecule viewed approximately down the C_2 axis of symmetry.

Table X. Comparison of Structural and ^{13}C NMR Data for Selected Diazoalkane Transition-Metal Complexes and Free Diazoalkanes

compd	M-N, Å	N-N, Å	N-C, Å	M-N-N, deg	N-N-C, deg	δ(ipso C)	ref
9-diazofluorene		1.126 (4)	1.323 (4)		179.6 (3)	*j*	*a*
diphenyldiazomethane						65.5	*b*
$Mo(O\text{-}t\text{-}Bu)_4(NNCPh_2)$	1.797 (3)	1.314 (4)	1.312 (5)	168.2 (3)	122.5 (3)	167.2	*b*
$Mo_2(O\text{-}i\text{-}Pr)_6(NNCPh_2)_2(py)$	1.76 (1)	1.319 (12)	1.287 (14)	164.4 (8)	123.8 (9)	152.2	*b*
	1.78 (1)	1.297 (11)	1.310 (13)	155.3 (7)	121.6 (9)	149.9	
$W_2(O\text{-}t\text{-}Bu)_6(\mu\text{-}NNC(C_6H_4Me)_2)_2$	1.942 (11) 1.991 (11)	1.410 (16)	1.264 (18)	*i*	136.6 (9)	159.3	*b*
$Cp_2Mo_2(CO)_3(CPh_2)(NNC(C_6H_4Me)_2)$	1.741 (10)	1.323 (12)	1.318 (13)	174.7 (9)	121.1 (10)	163.8	*c*
$Cp_2Mo_2(CO)_4(\mu\text{-}NNCPh_2)$	1.914 (3) 2.083 (8)	1.352 (10)	1.279 (12)	*i*	122.6 (9)	93.7	*d*
$[WBr(NNCMe_2)(dppe)_2]^+Br^-$	1.74 (1)	1.34 (2)	1.28 (2)	171 (1)	124 (1)	*j*	*e*
$[WBr(NNCH(CH_2)_3OH)(dppe)_2]^+PF_6^-$	1.78 (1)	1.31 (2)	1.29 (4)	172 (1)	116 (1)	171.4	*f*
$IrCl(NNC_5Cl_4)(PPh_3)_2$	1.819 (6)	1.171 (8)	1.346 (10)	174.9 (6)	141.0 (7)	*j*	*g*
$CpMn(CO)_2(NNC(COOMe)_2)$	1.796 (5)	1.165 (7)	1.351 (8)	176.9 (4)	150.5 (4)	*j*	*h*

[a] Tulip, T. H.; Corfield, P. W. R.; Ibers, J. A. *Acta Crystallogr., Sect. B* **1978**, *B34*, 1549. [b] This work. [c] Reference 7b. [d] Reference 7a. [e] Reference 19. [f] Chatt, J.; Bevan, P. C.; Head, R. A.; Hitchcock, P. B.; Leigh, G. J. *J. Chem. Soc., Chem. Commun.* **1976**, 509. [g] Schramm, D. K.; Ibers, J. A. *J. Am. Chem. Soc.* **1978**, *100*, 2932. [h] Hermann, W. A.; Kriechbaum, G.; Ziegler, M. L.; Wulknitz, P. *Chem. Ber.* **1981**, *114*, 276. [i] Not pertinent. [j] Not reported.

of 121°, implies a significant contribution of the resonance structure depicted by III.

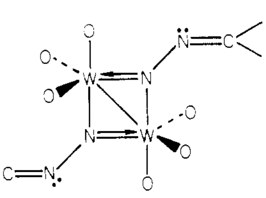

III

The positioning of the $C(p\text{-tol})_2$ group is to the same side of the $W_2(\mu\text{-}N)_2$ plane, and the molecule has crystallographically imposed C_2 symmetry. A stereoview of the molecule down the C_2 axis of symmetry is given in Figure 4.

Comparison with Related Transition-Metal Diazoalkane Complexes. Structural data for the new diazoalkane complexes are compared with those from previously reported studies in Table X. For the terminal $NNCAr_2$ ligands the characteristic short M–N and long N–N distances find a parallel with the related observations of Chatt et al. and Curtis and Messerle. The $\mu\text{-}NNCAr_2$ ligands in $Cp_2Mo_2(CO)_4(NNCAr_2)$ and $W_2(O\text{-}t\text{-}Bu)_6(NNCAr_2)_2$ are also similar. An interesting aspect of this work is that the new compounds provide examples of diazoalkane adducts involving metal atoms in their middle to higher oxidation states, which contrasts with previously known complexes involving metal atoms in lower oxidation states. Of course, assignment of oxidation state involves a formalism of electron counting. However, the structural assignment of an $NNCAr_2^{2-}$ ligand based on M–N and N–N distances leads to Mo^{6+} in $Mo(O\text{-}t\text{-}Bu)_4(NNCAr_2)$ vs. Ir^+ and Mn^+ in $IrCl(NNC_5Cl_4)(PPh_3)_2$ and $CpMn(CO)_2(NNC(COOMe)_2)$, respectively. This provides yet a further example of the reducing power (ease of oxidation) of $M_2(OR)_6$ compounds.[8]

NMR Studies. $Mo(O\text{-}t\text{-}Bu)_4(NNCPh_2)$. At +16 °C, 220 MHz, the ^1H NMR spectrum of $Mo(O\text{-}t\text{-}Bu)_4(NNCPh_2)$ shows only one *tert*-butyl signal, but on cooling of the sample to −40 °C this signal splits into two signals in the ratio 3:1, consistent with the adoption of a trigonal-bipyramidal structure having the $NNCAr_2$ ligand in an axial site. ^{13}C NMR data obtained at room temperature at 90 MHz are also consistent with a static (NMR time scale) structure. Clearly the trigonal-bipyramidal geometry is significantly favored over a square-based pyramid with the $NNCAr_2$ ligand in the axial position. This can reasonably be understood in terms of maximizing ligand to metal d π-bonding. In a square-based pyramid molybdenum has only d_{xz}, d_{yz}, and d_{xy} orbitals

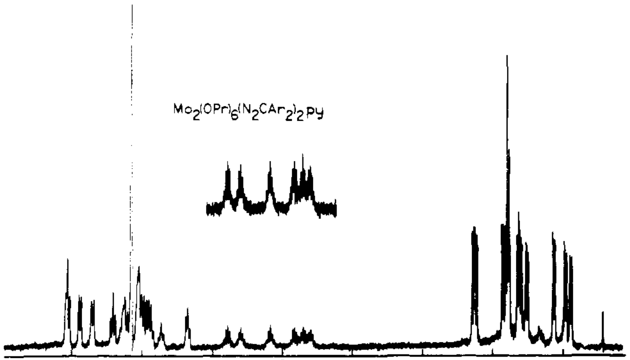

Figure 5. ^1H NMR spectrum of $Mo_2(O\text{-}i\text{-}Pr)_6(NNCPh_2)_2(py)$ recorded in toluene-d_8 at +16 °C, 220 MHz.

available for L–Mo d π-bonding, but the trigonal-bipyramidal geometry allows molybdenum to use d_{xz}, d_{yz}, d_{xy}, and $d_{x^2-y^2}$ atomic orbitals.

$Mo_2(OR)_6(NNCAr_2)_2L$ compounds have ^1H NMR spectra at room temperature that are consistent with expectations based on the solid-state molecular structure found for R = *i*-Pr, Ar = Ph, and L = py. Specifically, there are six different OR groups. The ^1H NMR spectrum of $Mo_2(O\text{-}i\text{-}Pr)_6(NNCPh_2)_2(py)$ is shown in Figure 5. There are six septets for the methyne resonances and twelve overlapping doublets for the isopropyl methyls. The latter arise because the isopropyl methyl groups of each O-*i*-Pr ligand are diastereotopic. The neopentoxy compounds show six *tert*-butyl-group resonances of equal intensity and six overlapping AB quartets for the methylene protons. When L = $HNMe_2$, the dimethylamino methyl protons appear as two doublets since the methyl groups are diastereotopic. When the temperature is raised to ca. 90 °C, the signals broaden and start to coalesce, consistent with the onset of rapid RO group site exchange. When Ar = phenyl, the phenyl signals coalesce, implying phenyl group exchange. Evidently the fluxional process makes both ends of the molecule equivalent, but it is not necessary to invoke terminal $\rightleftharpoons$ bridge bonding for the $NNCAr_2$ ligands.

$W_2(O\text{-}t\text{-}Bu)_6(NNCAr_2)_2$. The ^1H NMR spectrum of $W_2(O\text{-}t\text{-}Bu)_6(NNCPh_2)_2$ in toluene-d_8 at 220 MHz shows three O-*t*-Bu groups in the integral ratio 1:1:1 and two types of phenyl groups. Again this is consistent with expectations based on the solid-state molecular structure, which has C_2 symmetry. It should be noted, however, that this is also consistent with a molecule having C_2 symmetry with one CPh_2 lying above the central $W_2(\mu\text{-}N)_2$ plane and one lying below this plane. NMR spectroscopy cannot distinguish between these isomers. Since the N–N distance of 1.410 (16) Å corresponds to a single-bond distance, we infer that the barrier to interconversion is steric and not electronic. It can be noted that Chatt et al.[19] observed two Me signals (1:1) for the complex $[WBr(NNCMe_2)(dppe)_2]^+Br^-$, where dppe = $Ph_2PCH_2CH_2PPh_2$, and suggested that this was due to steric constraints imposed by the phenyl groups of the dppe ligand.

^{13}C NMR studies on the above were also supportive of the structural conclusions deduced from ^1H NMR spectroscopy. The ipso-carbon resonances, $\delta(NNC)$, occured in the range 160–170 ppm downfield from Me_4Si. This appears typical of earlier findings (see Table X) with the exception of $\delta(NNC)$ = 93.7 reported for $Cp_2Mo_2(CO)_4(\mu\text{-}CNNPh_2)$.

Because of the possibility that the N_2CAr_2 compounds could be precursors of μ-CAr_2 compounds (intermediates) which were not isolated in these reactions, we prepared $Ph_2{}^{13}CN_2$ and studied its reactions with $M_2(OR)_6$ compounds. This allowed unambiguous assignment of the ipso carbons and allowed us to follow, by ^{13}C NMR spectroscopy, reactions that failed to give crystalline products. For example, when $Ph_2{}^{13}CN_2$ was allowed to react with $Mo_2(OCH_2\text{-}t\text{-}Bu)_6$ in the absence of L in toluene-d_8, carbon resonances were seen at δ = 160.6, 166.6, 168.4, and 171.4, all of which can be assigned to coordinated diazoalkane ligands; cf. for the free diazoalkane $\delta(Ph_2{}^{13}CN_2)$ = 65.5. $W_2(O\text{-t-}Bu)_6(NNCPh_2)_2$ is unstable in toluene-d_8 at temperatures above +80 °C, and several ^{13}C signals are seen in the range observed for ipso-carbon atoms of coordinated diazoalkane ligands. None corresponded to $Ph_2C{=}CPh_2$ or a $W{=}CPh_2$ group, which would have shown $J_{W-C} \sim 150$ Hz.

Concluding Remarks

The reactions between $M_2(OR)_6$ and Ar_2CN_2 compounds may be viewed as redox reactions in which the dinuclear center is oxidized and the diazoalkane is reduced to a 2– ligand. The different isolable products reflect the steric constraints of the systems and their willingness to crystallize from hydrocarbon solutions. The cleavage of the Mo≡Mo bond in reactions involving $Mo_2(O\text{-}t\text{-}Bu)_6$ and Ph_2CN_2 has a parallel in reactions involving molecular oxygen.[10] A direct synthesis of $Mo(O\text{-}t\text{-}Bu)_4(NNCPh_2)$ from the reaction between $Mo(O\text{-}t\text{-}Bu)_4$ and N_2CPh_2 is also noteworthy in this regard and parallels the synthesis of $MoO(OR)_4$ compounds.[10] At this time the new compounds are rare examples of stable diazoalkane transition-metal complexes where the metal atoms are in relatively high oxidation states. We have found no evidence for the facile elimination of N_2 by either thermal or photochemical means. Presumably this reflects the high thermodynamic stability of the M–N multiple bonds in these compounds and the ability of the π-donor alkoxy ligands to stabilize the metal atoms in their higher oxidation states. Though steric factors at the dimetal center may impede formation of an intermediate of the type depicted by IV, it seems unlikely that this is the limiting factor with respect to evolution of N_2 especially since aryl azides react rapidly with $M_2(OR)_6$ compounds with the evolution of N_2 and an intermediate of similar geometry is anticipated.[18]

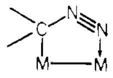

IV

Experimental Section

General Procedures. All preparations and procedures were carried out under a dry and oxygen-free atmosphere with standard Schlenk techniques or a Vacuum Atmospheres Co. Dri-Lab assembly. ^1H NMR spectra were recorded on a Varian HR 220 spectrometer. ^{13}C NMR spectra were recorded on a Nicolet 360 spectrometer. Infrared spectra were obtained from Nujol mulls between CsI plates with a Perkin-Elmer 283 spectrophotometer. Elemental analyses were performed by Alfred Bernhard Laboratorium, Elbach, West Germany, using drybox sampling techniques.

Materials. Dimetal hexaalkoxides were prepared as previously described.[20,21] Diphenyldiazomethane was prepared by reaction of benzophenone and hydrazine, followed by crystallization from 2-propanol. The hydrazone was dissolved in pentane and oxidized with mercuric oxide. The solution was dried with $MgSO_4$, filtered, and stored at –15 °C prior to use. The other diazoalkanes were prepared in a similar manner from the respective ketones.[22,23] *n*-BuLi in hexane was purchased from Alfa.

Syntheses. $Mo_2(O\text{-}i\text{-}Pr)_6[(C_6H_5)_2CNN]_2(py)$. $Mo_2(O\text{-}i\text{-}Pr)_6$ (300

---

(19) Chatt, J.; Head, R. A.; Hithcock, P. B.; Hussain, W.; Leigh, G. J. *J. Organomet. Chem.* **1977**, *133*, C1.

(20) Chisholm, M. H.; Cotton, F. A.; Murillo, C. A.; Reichert, W. W. *Inorg. Chem.* **1977**, *16*, 1801.

(21) Akiyama, M.; Chisholm, M. H.; Cotton, F. A.; Extine, M. W.; Haitko, D. A.; Little, D.; Fanwick, P. E. *Inorg. Chem.* **1979**, *18*, 2321.

(22) Smith, L. I.; Howard, K. L. "Organic Syntheses"; Wiley: New York, 1955; Collect. Vol. III.

(23) Hillhouse, G. L.; Haymore, B. L. *J. Am. Chem. Soc.* **1982**, *104*, 1537.

Table XI. Summary of Crystallographic Data

	a	*b*	*c*
fw	1013.98	1337.14	582.63
space group	$P2_1$	$C2/c$	$P\bar{1}$
a, Å	12.512 (8)	23.672 (5)	17.652 (10)
b, Å	14.795 (9)	12.214 (2)	12.366 (6)
c, Å	14.099 (8)	21.221 (6)	9.060 (3)
α, deg			76.95 (3)
β, deg	109.51 (2)	97.24 (1)	87.92 (3)
γ, deg			124.92 (2)
Z	2	4	2
V, Å^3	2459.98	6086.47	1545.38
d(calcd), g/cm^3	1.369	1.459	1.252
cryst size, mm	0.18 × 0.17 × 0.23	0.08 × 0.06 × 0.10	0.28 × 0.30 × 0.38
cryst color	black	dark green	black
radiation	Mo Kα (λ = 0.710 69 Å); graphite monochromator		
linear abs coeff, cm^{-1}	5.457	39.055	4.445
transmission factors	no abs cor	0.459–0.673	no abs cor
t, °C	−162	−165	−164
instrument	Picker 4-circle diffractometer, locally modified and interfaced		
detector aperture	3.0 mm wide × 4.0 mm high; 22.5 cm from crystal		
sample to source dist, cm	23.5		
takeoff angle, deg	2.0	2.0	2.0
scan speed, deg/min	3.0	5.0	4.0
scan width, deg	2.0 + 0.692 tan θ	1.8 + 0.692 tan θ	1.7 + 0.692 tan θ
bkgd counts, s at each end of scan	5	3	3
2θ range, deg	6–40	6–45	6–40
data collcd, total	3979	4042	3509
no. of unique data	3373	2832	2885
no. of unique data with $F_o > 2.33\sigma(F_o)$	3143	2228	2565
R(*F*)	0.051	0.053	0.033
$R_w(F)$	0.053	0.048	0.032
goodness of fit	1.028	1.408	0.896
largest Δ/σ	0.05	0.05	0.05

[a] $Mo_2(O\text{-}i\text{-}Pr)_6(NNCPh_2)_2(C_6H_5N)$. [b] $W_2(O\text{-}t\text{-}Bu)_6(NNC(p\text{-}tol)_2)_2$. [c] $Mo(O\text{-}t\text{-}Bu)_4(NNCPh_2)$.

mg, 0.549 mmol) was suspended in hexane (10 mL). Pyridine (3 mL) was added, and the solution was then cooled to −78 °C. A hexane solution of $(C_6H_5)_2CNN$ ($1^1/_2$ mL; 0.77 M) was added via syringe, causing an immediate color change from black to green. The solution was warmed to room temperature and the solvent removed in vacuo. The oily residue was dissolved in hexane (5 mL) and cooled to −15 °C to produce black crystals of $Mo_2(O\text{-}i\text{-}Pr)_6[(C_6H_5)_2CNN]_2(py)$ suitable for single-crystal X-ray structural determination and analysis. Yield: 35%.

^1H NMR data (obtained from benzene-d_6 solution at 16 °C and reported relative to Me_4Si): δ 0.80 (d, 3 H), 0.95 (d, 3 H), 1.20 (d, 3 H), 1.50 (d, 3 H), 1.60 (d, 3 H), 1.63 (d, 3 H), 1.83 (unresolved doublets, 6 H), 1.85 (d, 3 H), 1.89 (d, 3 H), 2.11 (d, 3 H), 2.20 (d, 3 H), 4.60 (sep, 1 H), 4.68 (sep, 1 H), 4.83 (sep, 1 H), 5.15 (sep, 1 H), 5.63 (sep, 1 H), 5.83 (sep, 1 H), 6.41, 6.61–8.1 (multiplets).

IR data: 1601 (w), 1550 (s), 1375 (s), 1330 (m), 1250 (m), 1150 (m), 1105 (s), 1062 (w), 1020 (m), 965 (s), 930 (m), 820 (w), 790 (w), 760 (w), 680 (m) cm^{-1}.

Anal. Cacld for $Mo_2(O\text{-}i\text{-}Pr)_6(NNCPh_2)_2(py)$: C, 58.1; H, 6.61; N, 6.91. Found: C, 58.7; H, 6.77; N, 6.74.

The compounds of general formula $Mo_2(OCH_2\text{-}t\text{-}Bu)_6[R(C_6H_5)CNN]_2L$ were synthesized in a similar manner.

$Mo_2(OCH_2\text{-}t\text{-}Bu)_6[H(C_6H_5)CNN]_2(py)$. ^1H NMR data (recorded in benzene-d_6 at 16 °C and reported relative to Me_4Si): δ 1.01 (s, 9 H), 1.10 (s, 9 H), 1.35 (s, 9 H), 1.43 (s, 18 H), 1.55 (s, 9 H), 3.1–5.45 (unresolved AB quartets), 6.55–7.90 (multiplets), 8.28 (s, 1 H), 9.05 (s, 1 H), 9.18 (d, 2 H).

IR data: 1600 (w), 1550 (m), 1382 (m), 1350 (m), 1255 (m), 1195 (s), 1120 (s), 1035 (m), 1015 (m), 962 (s), 899 (s), 795 (m), 684 (m), 640 (s), 595 (s), 420 (m), 432 (w) cm^{-1}.

Anal. Calcd for $Mo_2(OCH_2\text{-}t\text{-}Bu)_6(PhHCNN)_2(py)$: C, 57.17; H, 8.06; N, 6.80. Found: C, 57.52; H, 7.22; N, 6.61.

$Mo_2(OCH_2\text{-}t\text{-}Bu)_6[(C_6H_5)_2CNN]_2(py)$. ^1H NMR data (obtained from benzene-d_6 solution at 16 °C and reported relative to Me_4Si): δ 1.06 (s, 9 H), 1.12 (s, 9 H), 1.28 (s, 9 H), 1.43 (s, 18 H), 1.58 (s, 9 H), 3.0, 3.35, 4.0–4.5, 4.8–5.2 (unresolved AB quartets, 12 H), 6.45, 6.78–8.05 (multiplets, 20 H).

IR data: 1602 (w), 1560 (s), 1375 (s), 1321 (w), 1253 (w), 1069 (w), 1050 (s), 1012 (s), 952 (w), 762 (m), 718 (w), 685 (m), 630 (s) cm^{-1}.

$Mo_2(OCH_2\text{-}t\text{-}Bu)_6[(C_6H_5)_2CNN]_2(HNMe_2)$. ^1H NMR data (obtained from benzene-d_6 solution at 16 °C and reported relative to Me_4Si): δ 1.07 (s, 9 H), 1.19 (s, 9 H), 1.26 (s, 9 H), 1.29 (s, 9 H), 1.34 (s, 9 H), 1.39 (s, 9 H), 1.89 (d, 3 H), 2.09 (d, 3 H), 3.8 (unresolved multiplet, 1 H), 3.9–4.9 (AB quartets, 12 H), 6.65–7.95 (multiplets, 20 H).

^{13}C NMR data (obtained from benzene-d_6 solution at 16 °C and reported relative to Me_4Si): δ 23.19–27.53 ($OCH_2C(CH_3)_3$), 34.0, 35.0–35.05 ($OCH_2C(CH_3)_3$), 42.0, 43.2 ($HN(CH_3)_2$), 79.0, 79.05, 82.0, 85.13–85.20 ($OCH_2C(CH_3)_3$), 128.0–130.0, 136.7–137.0 (C_6H_5), 149.9, 152.2 ($(C_6H_5)_2CNN$).

IR data: 1430 (m), 1390 (w), 1330 (w), 1300 (w), 1200 (s), 1080 (s), 1012 (w), 998 (w), 917 (s), 862 (s), 742 (w), 710 (w), 688 (w), 632 (w), 580 (m), 546 (m), 470 (w), 382 (w) cm^{-1}.

Anal. Calcd for $Mo_2(OCH_2\text{-}t\text{-}Bu)_6(NNCPh_2)_2(HNMe_2)$: C, 60.68; H, 8.11; N, 6.10. Found: C, 60.66; H, 8.05; N, 5.53.

$Mo(O\text{-}t\text{-}Bu)_4[(C_6H_5)_2CNN]$. $Mo_2(O\text{-}t\text{-}Bu)_6$ (670 mg, 1.06 mmol) was suspended in hexane (5 mL). A pentane solution of $(C_6H_5)_2CNN$ (4 mL; 0.7 M) was added by syringe. The solution was cooled to −15 °C, producing large black crystals of $Mo(O\text{-}t\text{-}Bu)_4(C_6H_5)_2CNN$, which were collected by filtration and dried in vacuo. These crystals were suitable for single-crystal structural studies and further analyses. Yield: 15%.

Alternate Synthesis. $Mo(O\text{-}t\text{-}Bu)_4$ (800 mg; 2.60 mmol) was suspended in hexane (5 mL). A pentane solution of $(C_6H_5)CNN$ (2.6 mL; 0.8 M) was added by syringe. The solution immediately turned black. After stirring for 10 min, the solution was cooled to −15 °C, producing black crystals of $Mo(O\text{-}t\text{-}Bu)_4(C_6H_5)_2CNN$, which were filtered and dried in vacuo. Yield: 40%.

^1H NMR data (obtained from toluene-d_8 solution at 16 °C and reported relative to Me_4Si): δ 1.68 (s, 36 H), 6.98–7.95 (multiplets, 10 H).

IR data: 1357 (s), 1335 (w), 1330 (w), 1230 (m), 1190 (m), 1163 (s), 1070 (w), 1020 (m), 978 (m), 930 (s), 900 (m), 838 (w), 780 (m), 770 (m), 762 (m), 720 (m), 688 (m), 648 (w), 606 (w), 572 (m), 530 (w), 474 (w), 380 (w) cm^{-1}.

^{13}C NMR data (obtained from benzene-d_6 solution at 16 °C and reported relative to Me_4Si): δ 31.95, 33.11 ($OC(CH_3)_3$), 79.67, 81.74 ($OC(CH_3)$), 128–132, 135.2, 136.9 (C_6H_5), 167.2 ($(C_6H_5)_2CNN$).

Anal. Calcd for $Mo(O\text{-}t\text{-}Bu)_4(NNCPh_2)$: C, 59.77; H, 7.97; N, 4.81. Found: C, 59.55; H, 7.44; N, 4.87.

$W_2(O\text{-}t\text{-}Bu)_6[(MeC_6H_4)_2CNN]_2$. $W_2(O\text{-}t\text{-}Bu)_6$ (1100 mg, 1.36 mmol) was suspended in pentane (5 mL). A solution of $(MeC_6H_4)_2CNN$ (12 mL, 0.2 M) was added via syringe. The solvent was reduced to approximately 5 mL, after which toluene (2 mL) was added. Slow cooling of this solution produced black crystals of $W_2(O\text{-}t\text{-}Bu)_6[(MeC_6H_4)_2CNN]_2$, which were isolated by filtration and dried in vacuo. These crystals were suitable for single-crystal X-ray structural studies and further analysis. Yield: 65%.

^1H NMR data (obtained from toluene-d_8 solution at 16 °C and reported relative to Me_4Si): δ 1.31 (s, 18 H), 1.88 (s, 18 H), 1.93 (s, 18 H), 2.09 (s, 6 H), 2.25 (s, 6 H), 6.98–7.42, 7.8–7.99 (overlapping AB quartets, 16 H).

IR data: 1610 (w), 1400 (w), 1232 (w), 1180 (s), 1168 (s), 1019 (w), 974 (s), 948 (s), 924 (s), 821 (m), 786 (w), 771 (w), 722 (s), 648 (w), 620 (w), 560 (w), 463 (w), 369 (w) cm^{-1}.

Anal. Calcd for $W_2(O\text{-}t\text{-}Bu)_6[(MeC_6H_4)_2CNN]_2(C_6H_{12})$: C, 53.88; H, 7.25; N, 4.43. Found: C, 54.06; H, 6.80; N, 4.14.

$W_2(O\text{-}t\text{-}Bu)_2[(C_6H_5)_2CNN]_2$ was synthesized in a similar manner. ^1H NMR data (obtained from toluene-d_8 solution at 16 °C and reported relative to Me_4Si): δ 1.31 (s, 18 H), 1.83 (s, 18 H), 1.88 (s, 18 H), 6.98–7.38, 7.88–8.08 (multiplets, 20 H).

^{13}C NMR data (obtained from benzene-d_6 solution at 16 °C and reported relative to Me_4Si): δ 31.76, 31.91, 32.20 ($OC(CH_3)_3$), 76.29, 80.09, 84.42 ($OC(CH_3)_3$), 126.9–129.3, 132.0, 137.16, 138.18, 141.58 (C_6H_5), 159.19, 159.35 ($(C_6H_5)_2CNN$).

IR data: 1530 (w), 1460 (s), 1375 (s), 1358 (m), 1345 (w), 1325 (w), 1308 (w), 1290 (w), 1262 (w), 1230 (m), 1160 (s), 1050 (w), 1020 (w), 973 (s), 956 (s), 947 (s), 921 (s), 781 (w), 772 (m), 768 (m), 730 (m), 717 (s), 699 (m), 689 (m), 641 (m), 608 (w), 566 (w), 547 (m), 520 (m), 491 (w), 460 (m), 370 (m), 348 (m), 310 (w) cm^{-1}.

Anal. Calcd for $W_2(O\text{-}t\text{-}Bu)_6(NNCPh_2)_2$: C, 50.26; H, 6.25; N, 4.68. Found: C, 49.94; H, 6.16; N, 4.68.

X-ray Structural Determinations. General operating facilities have been described previously.[24] Crystal data for the three compounds studied in this work are given in Table XI.

$Mo(O\text{-}t\text{-}Bu)_4(NNCPh_2)$. A systematic search of a limited hemisphere of reciprocal space revealed no systematic absences or symmetry, and the crystal was assigned a primitive triclinic cell. Solution and refinement of the structure confirmed the assignment.

The structure was solved by direct methods and Fourier techniques and refined by full-matrix least squares. All hydrogen atoms were located in a difference Fourier synthesis phased on the non-hydrogen atoms. Final least-squares included isotropic thermal parameters for hydrogen atoms and anisotropic thermal parameters for all non-hydrogen atoms.

A final difference Fourier synthesis was featureless, the largest peak being 0.3 e/Å^3.

$Mo_2(O\text{-}i\text{-}Pr)_6(NNCPh_2)_2(py)$. A search of a limited hemisphere of reciprocal space located diffraction maxima that could be indexed as monoclinic, space group $P2_1$ or $P2_1/m$. Statistical tests and the ultimate solution and refinement of the structure confirmed the noncentric $P2_1$ to be the proper choice.

The structure was solved by direct methods and Fourier techniques and refined by full-matrix least squares. All atoms were assigned anisotropic thermal parameters during refinement. A final difference Fourier synthesis indicated numerous peaks in the range 0.4–0.8 e/Å, many of which could be assigned as hydrogen atoms. Due to the fact that many of the hydrogen atoms were not visible, no attempt was made to include their contribution in the final refinement.

The coordinates given in the tables refer to the proper enantimorph for the chosen sample, based on a refinement using both forms.

$W_2(O\text{-}t\text{-}Bu)_6(NN(p\text{-}tol)_2)_2(n\text{-}hexane)$. No small crystals were available, and the sample studied was cleaved from a larger fragment and transferred to the goniostat, by the use of standard inert-atmosphere handling techniques. The crystal was characterized by a reciprocal lattice search technique and found to be monoclinic, space group $C2/c$.

The structure was solved by a combination of direct methods, Patterson functions, and Fourier techniques. Full-matrix refinement converged rapidly with isotropic thermal parameters for all non-hydrogen atoms. A difference Fourier synthesis located approximately half of the hydrogen positions, and all were included in further refinement using fixed idealized positions (thermal parameter = 1 + B_{iso}, d(C–H) = 0.95 Å). Attempts to refine the non-hydrogen atoms anisotropically failed as N(3), C(4)–C(6), C(10), C(12), C(13), and C(17) converged to nonpositive definite thermal parameters. While this behavior may be due to an improper absorption correction, it is possible that a slight disorder may be present in the N_2 ligand.

Final refinement included fixed hydrogens, anisotropic parameters for W, and isotropic parameters for all other atoms. A final difference Fourier synthesis was featureless, the largest peak being 1.22 e/Å^3 located at the metal position. A solvent molecule (hexane) was located at the origin, and the molecule lies on a twofold crystallographic axis. Carbon atoms numbered 34, 35, and 36 and hydrogen atoms 42–48 and their symmetry-related atoms are hexane.

Acknowledgment. We thank the National Science Foundation and the Wrubel Computing Center for support. A.L.R. is the 1982/83 Indiana University SOHIO Fellow.

Registry No. $Mo(O\text{-}t\text{-}Bu)_4[(C_6H_5)_2CNN]$, 90219-37-7; $Mo_2(O\text{-}i\text{-}Pr)_6[(C_6H_5)_2CNN]_2(py)$, 81534-66-9; $W_2(O\text{-}t\text{-}Bu)_6[(MeC_6H_4)_2CNN]_2$, 90245-15-1; $Mo_2(OCH_2\text{-}t\text{-}Bu)_6[H(C_6H_5)CNN]_2(py)$, 90219-38-8; $Mo_2(OCH_2\text{-}t\text{-}Bu)_6[(C_6H_5)_2CNN]_2(py)$, 90245-16-2; $Mo_2(OCH_2\text{-}t\text{-}Bu)_6[(C_6H_5)_2CNN]_2(HNMe_2)$, 90245-17-3; $W_2(O\text{-}t\text{-}Bu)_6[(C_6H_5)_2CNN]_2$, 90245-18-4.

Supplementary Material Available: Complete listings of atomic positional parameters, anisotropic and isotropic thermal parameters, bond distances, bond angles, and structure factor amplitudes and stereodiagrams (78 pages). Ordering information is given on any current masthead page. In microfiche form only, reports are available from the Indiana University Chemistry Library, Bloomington, IN 47405, at $2.50 per report. Request MSC Report No. 82057 for $Mo(O\text{-}t\text{-}Bu)_4(NNCPh_2)$, No. 81022 for $Mo_2(O\text{-}i\text{-}Pr)_6(NNCPh_2)_2(py)$, and No. 82029 for $W_2(O\text{-}t\text{-}Bu)_6(NNC(p\text{-}tol)_2)_2(C_6H_{14})$.

---

[24] Caulton, K. G.; Huffman, J. C.; Lewis, L. N. *Inorg. Chem.* **1980**, *19*, 2755.